FOREX Publication
Open Access | Rapid and quality publishing

International Journal of
Electrical and Electronics Research (IJEER)
Case Study | Volume 11, Issue 2 | Pages 272-282 | e-ISSN: 2347-470X

Integrated Energy Management System for Microgrid based on Renewable Energy Sources

Vinay Kumar Tatikayala[1], Shishir Dixit[2] and Yashwant Sawle[3*]
[1,2,3]Department of Electrical Engineering, Madhav Institute of Technology and Science, Gwalior, India, tatikayalavinay@gmail.com[1], Shishir.dixit1@gmail.com[2]

***Correspondence:** Yashwant Sawle; yashsawle@gmail.com

ABSTRACT- An effective energy management strategy is crucial to ensure highest system reliability, stability, operation efficiency and cost-effective operation of renewable energy sources based standalone microgrid. This paper presents an efficient energy management system for microgrid incorporated with Photovoltaic system, PMSG based wind turbine and energy storages including battery, fuel cell-Electrolyzer. Implemented hybrid modified invasive weed optimization with perturbed and observed method for PV systems to harvest maximum energy during partial shading condition. A sliding mode controller is implemented for boost converter to work as maximum power point tracker for wind turbine. Three solar plants and three wind farms are considered in this paper to establish 1 MW microgrid. Each wind farm is established with multiple wind turbines and similarly each solar plant having multiple PV modules. Each wind turbine and solar plant has their own inverter to synchronize at point of common coupling (PCC). Effective controllers are proposed to supply quality power at PCC under linear status and nonlinear status of single and three phase loads. Small size battery is considered to work under transient time and electrolyzer-fuel cell set will be working under steady state condition to reduce the cost of the system. TS-Fuzzy based controllers are designed for all the converters and implemented hardware-in-loop on a Real Time Simulator (RTS) by using OPAL RT technology/modules. The results unveiled that the RTS precisely emulate the dynamics of the microgrid with proposed controllers.

Keywords: Microgrid, Photovoltaic, PMSG, Wind, MPPT, MIWO, Fuel Cell, Electrolyzer, Battery, Power Quality, Energy Management System.

ARTICLE INFORMATION

Author(s):Vinay Kumar Tatikayala, Shishir Dixit and Yashwant Sawle;
Received: 20/12/2022; **Accepted**: 05/04/2023; **Published**: 18/05/2023;
e-ISSN: 2347-470X;
Paper Id: IJEER 2012-07;
Citation: 10.37391/IJEER.110205
Webpage-link:
https://ijeer.forexjournal.co.in/archive/volume-11/ijeer-110205.html

Publisher's Note: FOREX Publication stays neutral with regard to Jurisdictional claims in Published maps and institutional affiliations.

1. INTRODUCTION

The renewable energy sources (RES) based standalone microgrids are becoming popular in present days. Generation of electricity from RES is a solution to reduce global warming. Interconnecting more renewable energy sources with storage device can help establishing a more stable microgrid. The power generation of RES is always fluctuating due to weather conditions. An effective energy management system can help supplying quality power to consumers during fluctuations in generation and load. Among many renewable energy sources, photovoltaic (PV) based solar plant and permanent magnetic synchronous generator (PMSG) based wind power generation systems are more popular in establishing microgrids [1-3], especially in rural areas or the areas where grid is impractical to supply power to consumers, and some isolated places where considering only RES based power generation systems, a locally placed standalone microgrid system is popular. Usually loads where connected to common coupling point (PCC) are unbalanced, nonlinear and reactive power loads. These loads will lead poor power quality of other sensitive loads. In order to provide quality power to consumers, proper controllers are required to satisfy the requirements by the loads with respective to generation. To compensate the surplus power, a battery can be effectively working due to its fast response under rapid changes on either load or generation or in both sides. However, the big size batteries are costlier for supplying power to high loads and also require high maintenance. Hence, small size of battery is considered in this paper and electrolyzer – fuel cell set is considered for continuous operation to consume surplus power or reach load demand. The electrolyzer can split water into hydrogen and oxygen gases and these gases can be used to generate electricity through Fuel Cell (FC) [4-5]. The generated hydrogen and oxygen can be stored in respective tanks to use when load demand is high, hence, it is having reliable and stable operation. However, due to slow time response and dynamics of FC, a small size battery is considered to maintain load demand during transient time periods. Battery will stop discharging automatically once FC handles load demand.

2. SYSTEM DESCRIPTION

The microgrid consists of three numbers of wind farms, three numbers of solar plants, battery bank, electrolyzer, fuel cell and different kinds of loads is considered in this paper as shown in *figure 1*. All these components are connected to point of common coupling (PCC). Each solar plant consists of many PV arrays, similarly each wind farm consists of many PMSG units coupled with respective wind turbines. Single inverter can be sufficient for each wind farm as well as each solar system.

FOREX Publication
Open Access | Rapid and quality publishing
International Journal of Electrical and Electronics Research (IJEER)
Case Study | Volume 11, Issue 2 | Pages 272-282 | e-ISSN: 2347-470X

However, individual maximum power point tracker (MPPT) converters are used for each wind and PV units as shown in *figure 2*. The complete list of wind turbines and PV arrays used in respective generation units is listed in *table 1* for 1MW system. The battery is connected to PCC through separate inverter followed by bidirectional converter. Electrolyzer and FC are connected to a separate DC-bus through their respective DC-to-DC converters. However, the electrolyzer will not be operating when FC is in operation and vice versa. Hence single inverter is sufficient for integrating to PCC. Different kind of loads are connected to PCC and it is very important to synchronize all the inverters were connected to PCC to maintain power quality.

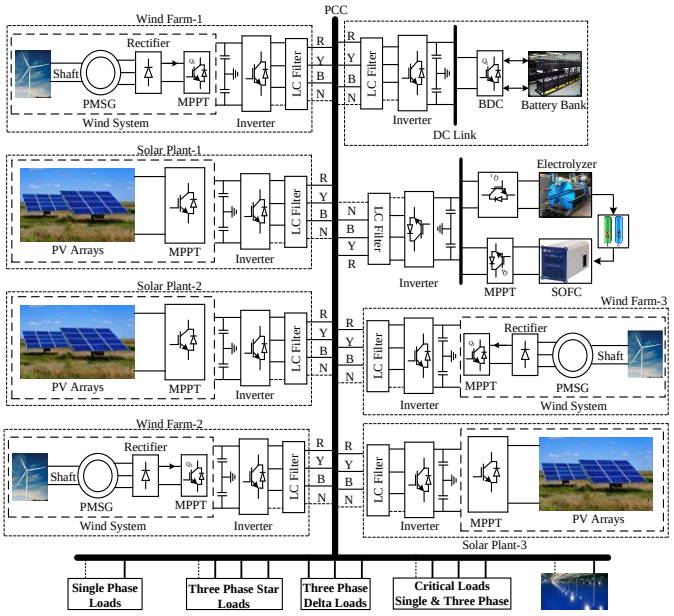

Figure 1: Renewable Energy Sources based Microgrid

Table 1: Ratings of wind farms and solar plants

No	Power station	Digit of 'N'	Power/one system	Capacity of plant (kW)
1	Wind Farm1	8	6.4	51.2
2	Wind Farm2	10	6.4	64.0
3	Wind Farm3	15	6.4	96.0
4	Solar Plant1	17	14.2	241.4
5	Solar Plant2	16	14.2	227.2
6	Solar Plant3	23	14.2	326.6

In order to obtain maximum efficiency of RES, effective MPPT algorithms are required for both wind and PV. Many algorithms are available to harvest maximum energy from wind turbines, however, they require speed sensors. A Sliding Mode Controller (SMC) based algorithm is implemented on the boost converter for extracting maximum power from PMSG which is directly coupled by shaft of wind turbine. Hence, voltage and currents of boost converter are sufficient to develop MPPT algorithm (i.e., SMC) for wind system. Moreover, conventional perturb and observe (P&O) algorithm fails to extract maximum power from PV under partial shading condition (PSC) [6-8]. In order to avoid this problem, the technique Modified Invasive Weed Optimization (MIWO) and P&O algorithm are hybridized for developing MPPT controller for boost converter of PV array.

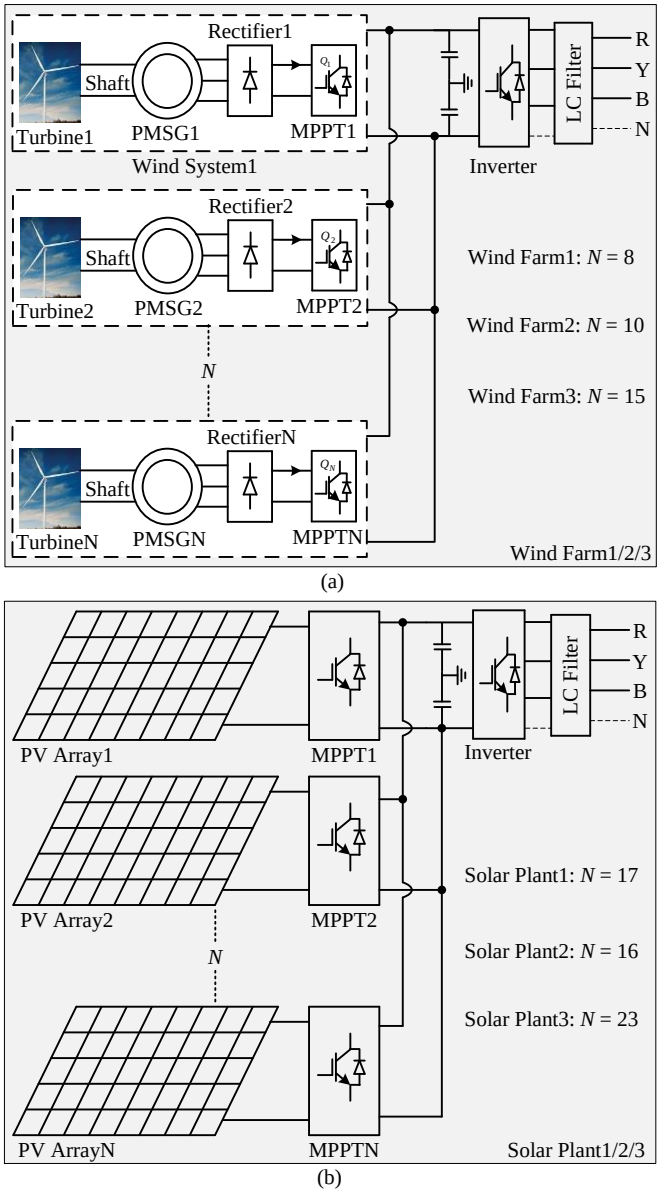

Figure 2: Configuration of (a) Wind Farm(s), (b) Solar Plant(s)

Similar kinds of systems are developed by many scholars, apart from many few important systems are listed in [2, 9-23]. In [2], authors proposed a voltage controller for wind and PV based standalone system and also considered battery, electrolyzer and FC. However, the components of system in [2] are connected to common DC bus. All components in this kind of systems are placed at same place and small rating of system. The authors in [9-11] presented the optimization procedure for renewable energy sources-based systems. However, in [9-11], authors did not address the energy management system and the system is connected with common DC bus. Hybrid renewable energy sources based standalone system is proposed for residential applications by authors in [12]. However, these kinds of

FOREX Publication
Open Access | Rapid and quality publishing
International Journal of Electrical and Electronics Research (IJEER)
Case Study | Volume 11, Issue 2 | Pages 272-282 | e-ISSN: 2347-470X

systems are applicable for small community and all sources are considered at same location. The authors in [13] proposed a single phase standalone system with different kinds of renewable energy sources. However, the system in [13] is limited to single phase and authors did not address electrolyzer and FC. The diesel generator-based standalone systems are proposed in [14-16]. However, application of these systems is limited and there was no information about the applicability of having sources in different locations. Moreover, authors in [14-16] did not provide discussion about FC and electrolyzer. The frequency control of standalone microgrid with renewable energy sources is presented in [17]. However, the sources in [17] are placed in same location, the authors also did not discuss the energy management system as well as applications of electrolyzer – FC. The MPPT of hybrid renewable energy sources based standalone microgrid is discussed in [18], however, authors did not address the energy management system as well as applications of electrolyzer – FC. The production of hydrogen and application of FC with renewable energy sources based standalone system are discussed by authors in [19-23]. However, the authors did not address the energy management systems and did not consider sources in various locations. It is very important to design proper energy management system in standalone microgrid that has sources in different locations.

3. DC SIDE CONTROLLERS

PMSG based wind energy to electricity conversion system is considered in this paper. Total 33 wind turbines are considered in this paper in three wind farms which are located in different places. Each wind farm is integrated with PCC with single inverter. Hence, it is very important to connect all PMSGs in each wind farm to a common DC-bus which is treated as the input of the respective inverter. However, due to variable wind speed, the output of all PMSGs cannot be connected directly. Hence the PMSG output is converted to DC through an uncontrolled three phase rectifier (diode). Output of each diode rectifier is connected to respective boost converter as shown in *figure 2* and SMC is implemented to work boost converter as MPPT converter of respective wind turbine. The controller of SMC is not required to sense the speed of wind turbine. The implemented SMC is shown in *figure 3* and the parameters involved in SMC are provided in *table 2*.

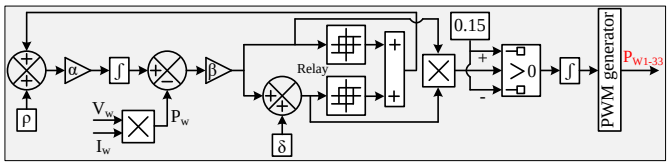

Figure 3: MPPT of wind turbine

Table 2: Parameters involved in SMC

S. No	Parameter	Value
1	ρ	0.1
2	α	80
3	β	0.03
4	δ	0.8

All boost converters used in wind farm(s) are connected to a common DC-link, hence generated power by all the PMSG can feed to microgrid by regulating DC-link voltage even under low wind speed. At the same time these boost converters can work as MPPT converters of respective wind turbines by controlling with SMC. Similarly, every solar plant established by connecting PV arrays/strings, and every array is connected to an individual MPPT converter. However, single inverter can manage to transfer total generated power of solar plant to Microgrid/PCC which can decrease complexity and price of complete system. The complete block diagram of PV array under partial shading and PV cell are shown in *figure 4 (a)* and *(b)* respectively.

The PV string is modeled by considering series connection of 22 number of PV modules to generate 660V at the maximum level of irradiance. The parameters of single PV module are listed in *table 3*. Each PV array designed by connecting three PV strings in parallel to decrease amount of MPPT devices to be used, hence it can be a solution for cost effective system. Therefore, a single DC-DC converter can work effectively as a MPPT converter for the whole PV array (i.e., for three PV strings). However, such a layout is having more chance to get partial shading conditions (PSCs). Under these circumstances, the designed MPPT mechanism must handle PSCs to harvest the maximum available energy. Two different patterns of PSC are listed in *table 4* and modeled based on the references [2-3, 12-14].

Table 3: Parameters of a PV Module

S. No.	Parameters	Values
1	Short-circuit current	8.01
2	Open circuit voltage	36.90
3	Voltage at MPP	30.30
4	Current at MPP	7.10

Table 4: Partial shading Conditions

Pattern	For one PV string irradiance in W/m^2
1	[1st *Partial shaded condition*]: **figure 5(b)** Modules: 1 to 3=1000; 4 to 8=800; 9 to 18=600; 19 to 22=400
2	[2nd *Partial shaded condition*]: **figure 5(b)** Modules: 1=1000; 2 to 4=800; 5 to 12=600; 13 to 22=400

The PV system can exhibit its maximum power by operating at a particular voltage level (V_{mpp}) as indicated in *figure 5(a)* under different level of irradiances. However, the conventional designed P&O technique fails to identify the best MPP location under the PSC due to existence of many local maximum points depicted in *figure 5(b)*. The voltage corresponding to the maximum power point achieved by P&O algorithm is stated by *equation (1)* [2-4].

$$V_{mpp}(i) = \Delta V \times \text{sign}\left(\frac{dP_{pv}}{dV_{pv}}\right) + V_{mpp}(i-1) \quad (1)$$

FOREX Publication
Open Access | Rapid and quality publishing
International Journal of Electrical and Electronics Research (IJEER)
Case Study | Volume 11, Issue 2 | Pages 272-282 | e-ISSN: 2347-470X

ΔV is the small step variation in voltage, *i* represent the iteration number.

During PSC, many local peaks of PV power points are existed, but one will become a global maximum power point (GMPP) among them which is like shown in *figure 5 (b)*. Traditional algorithm(s) (i.e., P&O and incremental conductance) may not guarantee for convergence to reach GMPP. Therefore, the modified invasive weed optimization (MIWO) algorithm is developed and integrated to P&O algorithm for finding the GMPP among all local peaks during PSCs. The characteristics of PV system under PSC are depicted in *figure 5 (b)*. The proposed MIWO based P&O algorithm can help to find GMPP by continues to update the V_{mpp} signal. The flow chart of hybrid P&O-MIWO is depicted in *i*.

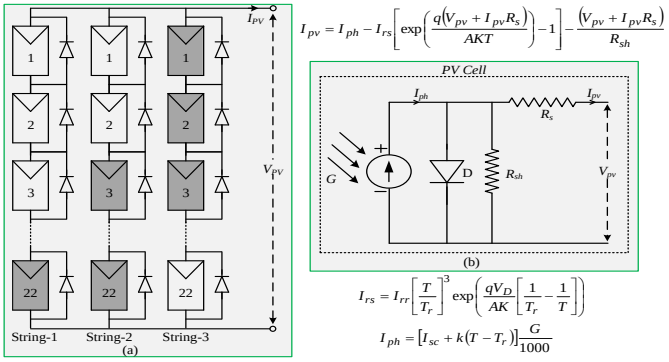

$$I_{pv} = I_{ph} - I_{rs}\left[\exp\left(\frac{q(V_{pv}+I_{pv}R_s)}{AKT}\right)-1\right]-\frac{(V_{pv}+I_{pv}R_s)}{R_{sh}}$$

$$I_{rs} = I_{rr}\left[\frac{T}{T_r}\right]^3 \exp\left(\frac{qV_D}{AK}\left[\frac{1}{T_r}-\frac{1}{T}\right]\right)$$

$$I_{ph} = [I_{sc} + k(T - T_r)]\frac{G}{1000}$$

Figure 4: Model of PV (a) system/array, (b). single cell

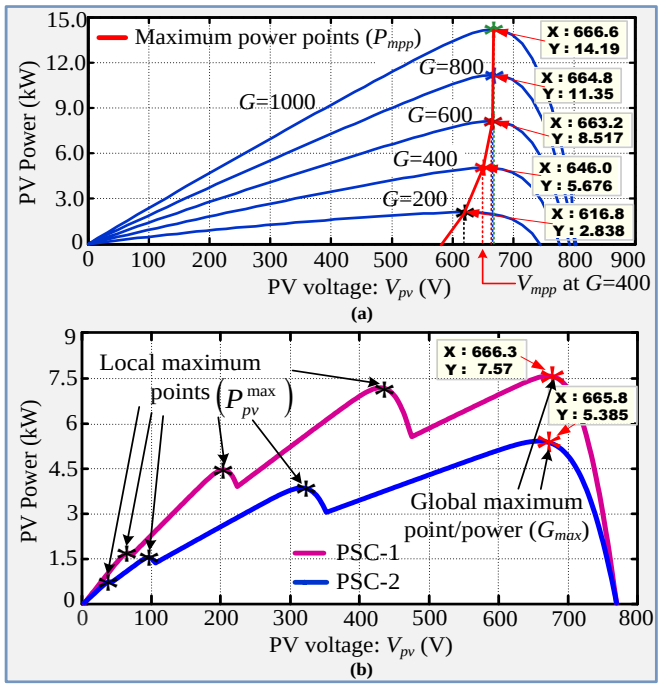

Figure 5: P-V curves under (a) symmetrical irradiance, (b) PSC

The reference voltage signal which is corresponding to maximum power point is generated by P&O-MIWO algorithm and compare with PV array voltage to generate duty cycle through PI/TS-Fuzzy controller as shown in *figure 7*. Individual MPPT controllers are designed to respective MPPT converters (*i.e.*, boost converter) of PV arrays as shown in *figure 2*.

The power generated by PV and wind depends on nature, hence energy storage devices are required to stabilize the power of the microgrid. Battery is one of the efficient energy storage devices, hence a battery bank is considered to maintain the power balance in microgrid. Individual battery bank is considered with own inverter for connecting to PCC. Moreover, to maintain charging and discharging properly a bidirectional DC-to-DC converter with proper controller is incorporated in this paper. The power balance is maintained by regulating voltage at DC-link with proposed controller as shown in *figure 8*. In order to protect the battery from over charging the controller is designed by considering state of charge (SoC) of battery.

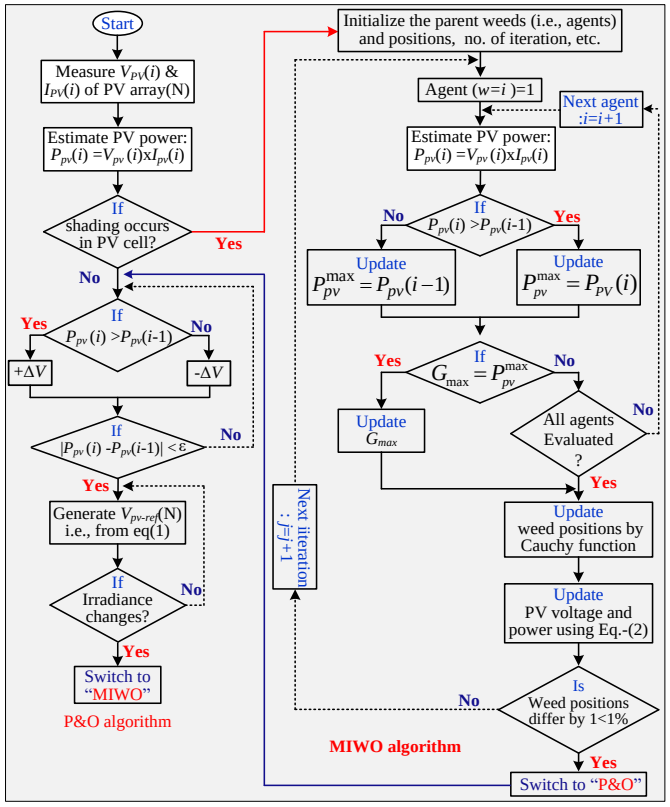

Figure 6: Flow chart of proposed P&O-MIWO algorithm for MPPT of PV array

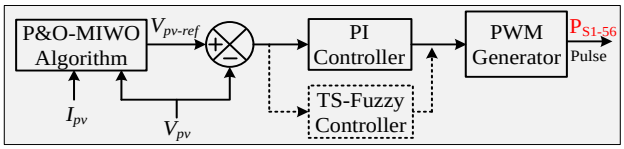

Figure 7: MPPT controller of boost converter for PV System

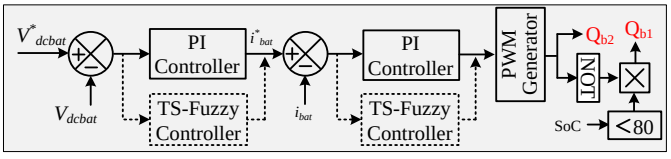

Figure 8: Controller for bidirectional DC-to-DC converter of battery

FOREX Publication
Open Access | Rapid and quality publishing
International Journal of Electrical and Electronics Research (IJEER)
Case Study | Volume 11, Issue 2 | Pages 272-282 | e-ISSN: 2347-470X

However, high capacity of batteries is required to maintain power balance of 1 MW microgrid which is costly and requires high maintenance. Hence, electrolyzer and Fuel Cell (FC) set are considered to handle deficiency of power between generation and load during steady state. Due to slow dynamic responses of electrolyzer and FC, the small capacity of battery can efficiently handle the power balance of microgrid during transient time periods due to its fast response. The electrolyzer need to operate at high current to produce more hydrogen and oxygen from water. Hence, electrolyzer is connected to DC-link through buck converter to maintain high current on electrolyzer side. Similarly, FC is operating at low voltage, hence boost converter is used to incorporate FC to DC-link. The common DC-link is used for electrolyzer-FC set as shown in *figure 1*. Either electrolyzer or FC will operate at the particular time depends on availability of power. The electrolyzer will operate if battery SOC reaches to 80%. The FC will operate if load demand is more than the generation from wind farms and solar plants. The controller for buck converter which is used to connect electrolyzer to DC-link is shown in *figure 9(a)* and controller for boost converter which is used to connect FC to DC-link is shown in *figure 9(b)*. The electrolyzer reference voltage is less as compared to DC-link voltage, hence flowing of current from DC-link to electrolyzer will increase. This increasing current can help to have high production of hydrogen and oxygen. These gases can be stored in respective cylinders, these can be utilized by FC to generate electricity when the generation is less than the load demand. From *figure 9(b)*, battery current will reach zero in steady state once FC current reach load demand. This can be achieved by considering battery current in designing the controller for boost converter of FC. The SoC is used in designing the controller of FC to stop the operation for electrolyzer when FC is in operation. Otherwise, electrolyzer will start to produce hydrogen and oxygen by consuming power from FC. Similarly the battery will be first priority to charge from surplus power hence the operation of electrolyzer is restricted till battery SoC reaches 80% by considering SoC limit in controller of buck converter (i.e., converter of electrolyzer). Single inverter is connected between DC-link of electrolyzer-FC set and PCC for respective power flow.

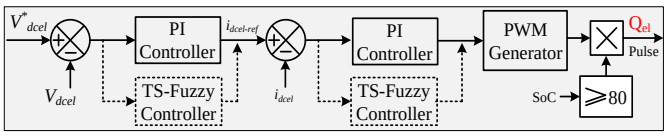

Figure 9(a): Controller for buck converter of electrolyzer

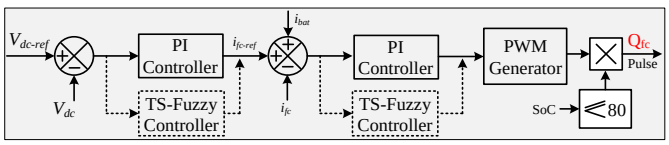

Figure 9 (b): Controller for boost converter of Fuel Cell

4. AC SIDE CONTROLLER

Major loads connected to microgrid are AC loads, nonlinear, single phase and reactive power loads. Hence, effective controllers are required for inverters connected to the PCC in order to maintain proper power quality. Single inverter is considered for individual solar plant and wind farm. Hence all PV arrays are coupled to common DC-link through their individual MPPT converters and similarly all wind generations also connected to their common DC-link voltage. However, individual inverters are considered for wind farms and solar plants, hence individual controllers are needs to be designed based on their objectives.

The controller of inverters which are associated with wind farms is shown in *figure 10*. The controller for these inverters is designed to transfer active power to PCC. Apart from these oscillations due to nonlinear and unbalanced load on PCC is restricted to enter into DC-link voltage. Because of these oscillations severe damage on PMSG shaft may happen [1]. Hence, the oscillating components in DQ are eliminated through proposed controller. Further, this inverter can supply balanced currents to PCC with the help of proposed controller. By comparing quadrature axis current with zero reference, the inverter can supply only active power to PCC which is generated from corresponding wind farm.

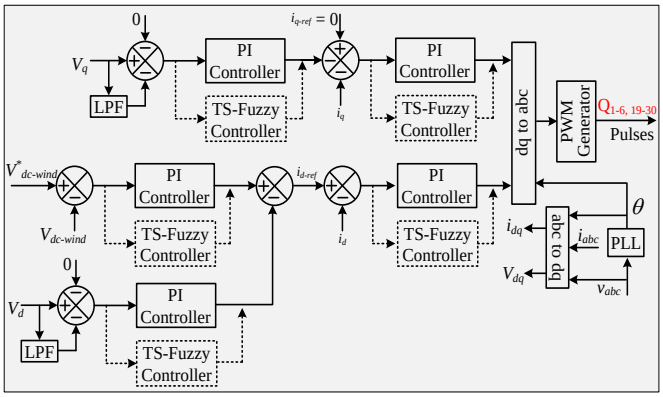

Figure 10: Controller of Inverter for wind farm

The compensation of reactive power is very important to maintain power quality at PCC. Hence, the three inverters which are associated with solar plants (Plant 1 to 3) are assigned to share compensation of reactive power which is required by load at PCC. The inverter controller is designed based on transferring active power generated by solar plant to PCC as well as sharing the compensation of reactive power. The reactive power sharing can be done by comparing RMS voltage to its reference value then generate reference reactive component of current. This reactive component of current further divided by number of solar plants (*i.e.*, 3 in this paper, N_{pv}=3). Therefore, the reactive power required by load can be compensated by sharing all the inverters that are associated with solar plants. The proposed controller of inverters associated with solar plants is shown in *figure 11*. Further, these controllers can regulate RMS voltage of PCC at its reference value. Even during night time or no irradiance period, inverters will work as DSTATCOM to compensate reactive power as well as regulating RMS voltage at PCC.

FOREX Publication
Open Access | Rapid and quality publishing
International Journal of Electrical and Electronics Research (IJEER)
Case Study | Volume 11, Issue 2 | Pages 272-282 | e-ISSN: 2347-470X

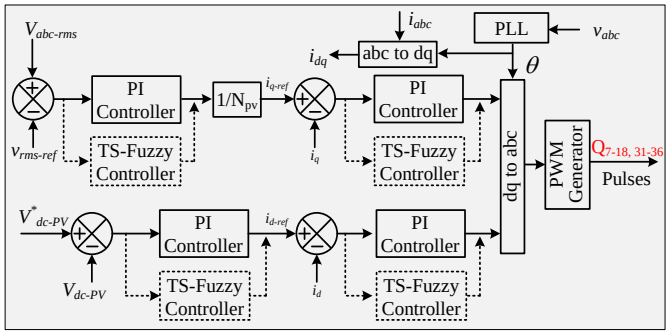

Figure 11: Controller of Inverter for Solar plant

The battery needs to work in transient time periods and it is associated with separate inverter followed by DC-to-DC bidirectional converter. The bidirectional converter can regulate its DC-link voltage, hence the inverter need to regulate AC output which is connected to PCC. The proposed inverter controller for battery is shown in *figure 12*. As it is standalone system, the frequency regulation is very important hence the flow of active power controller is designed by regulating frequency of PCC at its reference value. By taking this frequency, the other inverters will make synchronizing with PCC. The oscillations due to harmonics in generation currents (wind, PV and FC) are comparing with zero reference, hence, the controller can allow the harmonic component through this inverter to work as active power filter. The hysteresis current controllers are used to run the inverter as shunt active power filter.

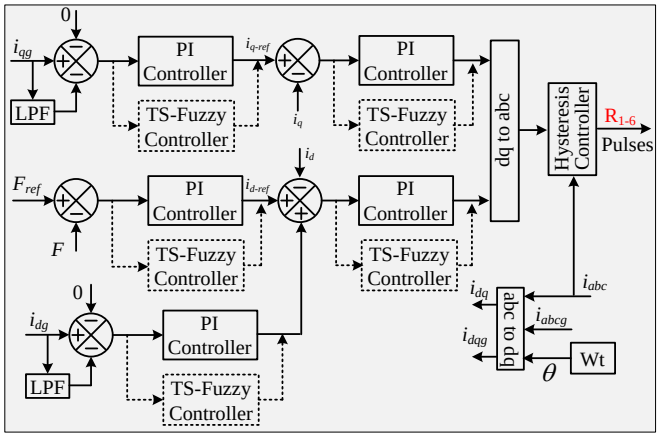

Figure 12: Controller of Inverter associated with battery

The inverter that is associated with electrolyzer-FC set is used to transfer surplus power to electrolyzer when load is more than the generation as well as to supply power from FC to PCC when load demand is more than the load. The power flow can be done by regulating DC-link voltage. Hence, DC-link voltage is considered while designing the controller and the same inverter is also used to compensate unbalanced load currents. This inverter can convert unbalanced current to DC when electrolyzer is under operation accordingly to compensate unbalanced load currents that exist due to unbalanced load at PCC. This can helps to flow balanced currents through PCC. Therefore, balanced currents can be produced by other inverters to PCC by generating unbalanced currents through inverter that is associated with electrolyzer-FC set. The proposed controller for inverter which is associated with electrolyzer-FC set is shown in *figure 13*.

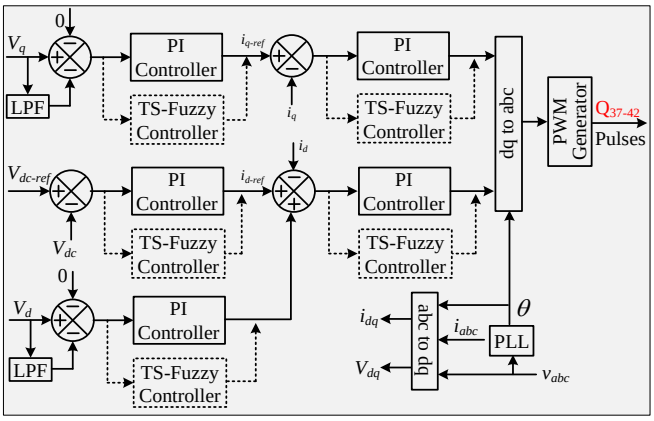

Figure 13: Controller of Inverter associated with FC-Electrolyzer

5. TS FUZZY CONTROLLER

The proportional plus integral controllers are tuned at particular instant, hence the same gains may not work properly during rapid changes in solar irradiance as well as sudden changes in load. Therefore, TS-Fuzzy controllers are implemented to produce smooth operation under rapid irradiance changes [4]. The procedure along with proper description of the TS-Fuzzy controller is provided here. The inputs of TS-Fuzzy controller are treated as error variations of voltage/current (x_i) and its derivative ($\dot{x}_i$) signals, as shown in *figure 14*. The fuzzification in the controller for two inputs is evaluated by respective membership functions (MFs) such as negative (N) and positive (P) that is displayed in *figure 14*. The MFs of x_i & $\dot{x}_i$ signals are represented by eq. (2) and eq. (3). The designed rules of the TS-Fuzzy controller are listed in *table-5*.

$$\mu_P(x_i)=\begin{cases}0, & x_i < L_1\\ \dfrac{x_i+L_1}{2L_1}, & -L_1 \le x_i \le L_1\\ 1, & x_i > L_1\end{cases} \text{ and}$$

$$\mu_N(x_i)=\begin{cases}1, & x_i < L_1\\ \dfrac{-x_i+L_1}{2L_1}, & -L_1 \le x_i \le L_1\\ 0, & x_i > L_1\end{cases} \qquad (2)$$

$$\mu_P(\dot{x}_i)=\begin{cases}0, & \dot{x}_i < L_2\\ \dfrac{\dot{x}_i+L_2}{2L_2}, & -L_2 \le \dot{x}_i \le L_2\\ 1, & \dot{x}_i > L_2\end{cases} \text{ and}$$

$$\mu_N(\dot{x}_i)=\begin{cases}1, & \dot{x}_i < L_2\\ \dfrac{-\dot{x}_i+L_2}{2L_2}, & -L_2 \le \dot{x}_i \le L_2\\ 0, & \dot{x}_i > L_2\end{cases} \qquad (3)$$

In *table 5*, Z_1, Z_2, Z_3, and Z_4characterize outputs of TS-Fuzzy process. 'K'denotes sampling instant. a_1, a_2, a_3, a_4 and

FOREX Publication
Open Access | Rapid and quality publishing
International Journal of Electrical and Electronics Research (IJEER)
Case Study | Volume 11, Issue 2 | Pages 272-282 | e-ISSN: 2347-470X

$a_5$designate the fuzzy constants. A generalized defuzzifiers of the controller's output(Y) is denoted by eq. (4).

$$Y = \frac{Z_1F_1 + Z_2F_2 + Z_3F_3 + Z_4F_4}{Z_1 + Z_2 + Z_3 + Z_4} \quad (4)$$

Where,

F_1= minimum { $\mu_p(\dot{x}_i)$, $\mu_p(x_i)$ },

F_2= minimum{ $\mu_N(\dot{x}_i)$, $\mu_p(x_i)$ },

F_3= minimum { $\mu_p(\dot{x}_i)$, $\mu_N(x_i)$ }, and

F_4= minimum { $\mu_N(\dot{x}_i)$, $\mu_N(x_i)$ }

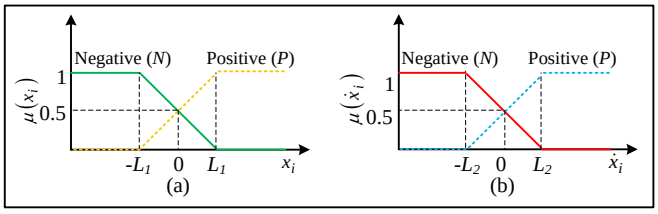

Figure 14: Membership functions of Fuzzy rules

Table 5: The TS-Fuzzy controller rules

Rule	x_i(k)	$\dot{x}_i$(k)	function
Rule1	*N*	*N*	$Z_1 = a_1x_i(k) + a_2\dot{x}_i(k)$
Rule2	*N*	*P*	$Z_2 = a_3Z_1$
Rule3	*P*	*N*	$Z_3 = a_4Z_1$
Rule4	*P*	*P*	$Z_4 = a_5Z_1$

6. RESULTS

The proposed Microgrid system presented in *figure 1* is implemented on a real-time simulator (RTS) platform using OPAL-RT technology. The configuration of Hardware-In-Loop (HIL) is attempted by interconnecting two OPAL-RT modules here. One unit serves as a microgrid block while other is used to build the controller as shown in in *figure 15*.

The HIL setup of proposed system is established by sending analogue signals from the OPAL RT1 unit to the controller unit (OPAL RT2). Similar way, the digital signals are coming to unit-1 from unit-2.

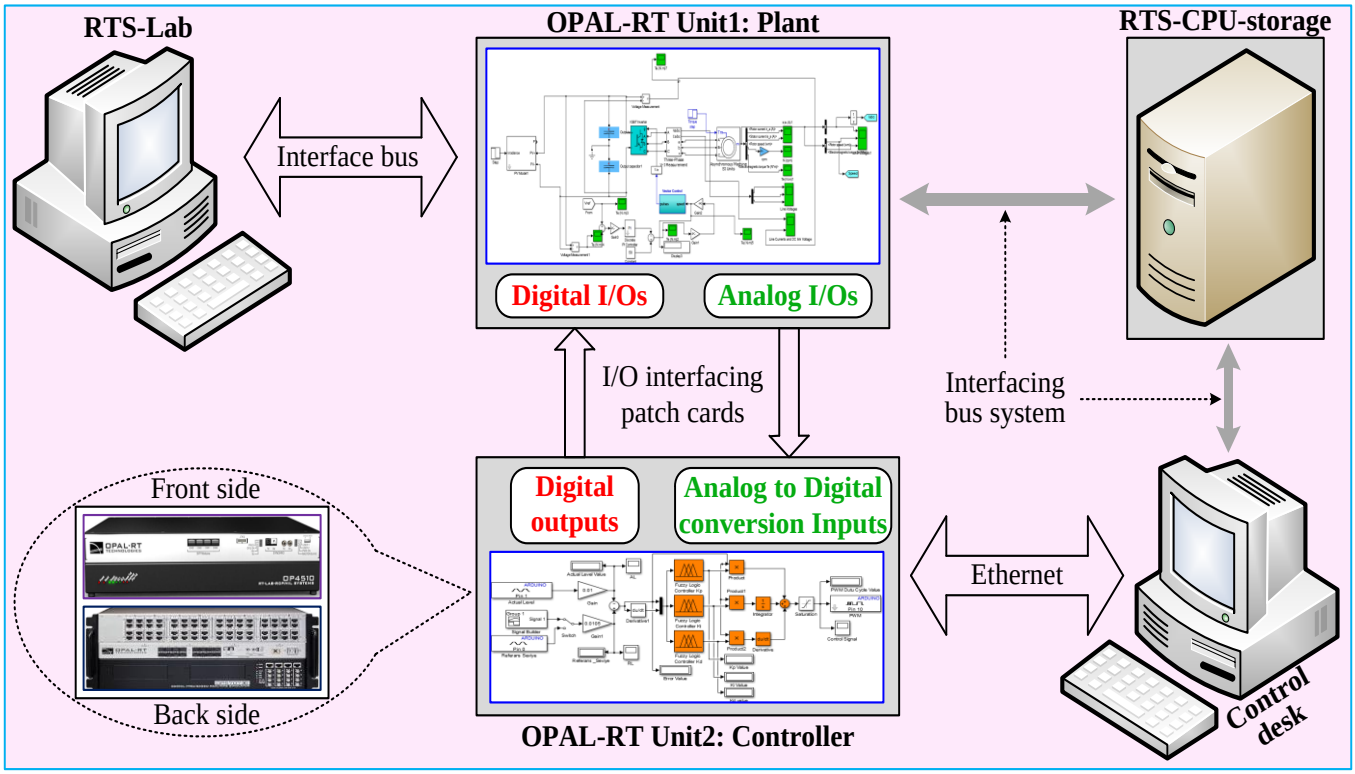

Figure 15: Configuration of OPAL-RT

In order to form Hardware – in- loop (HIL), the complete system needs to be divided into two parts. One is Plant and another one is controller. The plant model consists of all components including converters, sensors for voltage, current, SoC, etc. The controller unit consists of only controllers and output as digital signals for pulses. The plant is dumped in 'OPAL-RT'1 & other 'OPAL-RT'2 consists of controller block. The complete block representation with color coding of analog and digital signals for HIL is depicted in *figure 16*. The following case studies are investigated to evaluate the significance and verify the performance of the system.

FOREX Publication
Open Access | Rapid and quality publishing
International Journal of Electrical and Electronics Research (IJEER)
Case Study | Volume 11, Issue 2 | Pages 272-282 | e-ISSN: 2347-470X

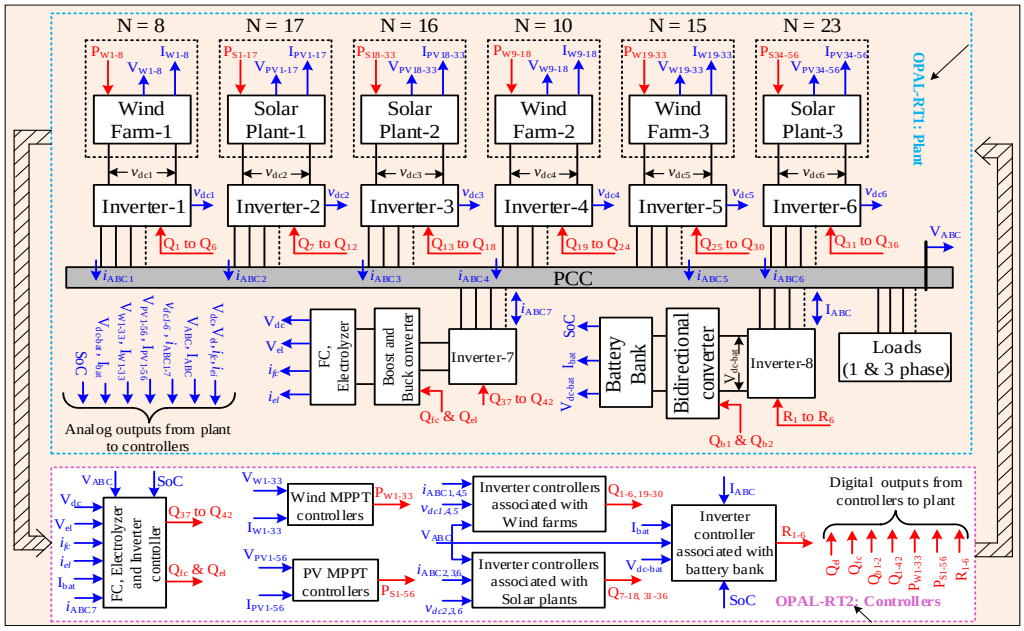

Figure 16: HIL Block diagram of proposed system

Case-A: MPPT Performance of PV System

The single PV array (i.e., three PV strings) is tested in this case under PSC and uniform irradiance. Initially assumed the irradiance at maximum and then drops at t=0.6sec to 900W/m^2. Corresponding responses of the system under this situation are presented in *figure 17*. The obtained DC-link voltage $V^*_{dc}(V_{mpp})$ is presented in *figure 17(b)*. V_{mpp} is obtained by implemented MPPT algorithms having ability to track, as discussed. The voltage at dc-link is slightly dropped due to decreasing in irradiance at *t*=0.6sec by the proposed MIWO-P&O algorithm as provided in *figure 17(b)*. The performance of MPPT algorithm is compared with another two optimization techniques: 1) Particle Swarm and P&O (PSO+P&O) [12], and 2) Grey Wolf and P&O (GWO+P&O) [13] to validate the effectiveness of proposed hybrid MIWO-P&O algorithm. Fig.17 represents the recommended MIWO-P&O has sufficient priority on dynamic response of V_{mpp}in factor of lower ripples and quick response compared to the other two optimization algorithms.

The power generated from single PV array in solar plant is as shown in *figure 17(c)*. It is clearly showing that more power can be extracted by using proposed MIWO-P&O technique due to generating smooth v_{mpp} signal. Voltage at DC-link of inverter used in solar plant is depicted in *figure 17(d)*. The permissible small voltage dip in DC-link voltage is occurred during changing in irradiance, however it is under limit.

The performance of proposed MIWO-P&O algorithm for MPPT is also tested under PSCs which are listed in *table 4*. The power obtained from PV system(s)/Array is shown in *figure 18(a)* and observed that the MIWO based algorithm can extract more as compared with GWO and PSO. Response of the MPP and its tracking time of PV are compared in *figure 18(b)*. The proposed MIWO-P&O utilizes only 57.0% of PSO's time in PSC1, and also extract somewhat more power in PSC1 and PSC2. It supports the argument that the MIWO-P&O performs better in PSCs.

Case-B: Performance of Wind turbine MPPT

Model of two mass wind turbine is designed for more realistic results from MPPT. Considered changes in wind speed from 12m/s to 7.0m/s at t=1.5 sec., and again increased from 7 m/s to 10 m/s at t=4 sec., as shown in *figure 19*. During these changes wind turbine torque is followed by reference torque that is estimated from wind turbine data [1, 3]. The response of reference torque and mechanical torque of the wind turbine is also depicted in *figure 19*. The torque gradually decrease when suddenly decrease in wind speed due to the effect of the two mass model. From 19, it can be observed that the wind turbine is operated at its maximum power point [1, 3]. The torque of the PMSG (*i.e.*, wind turbine) is followed by reference torque due to regulating current of boost converter.

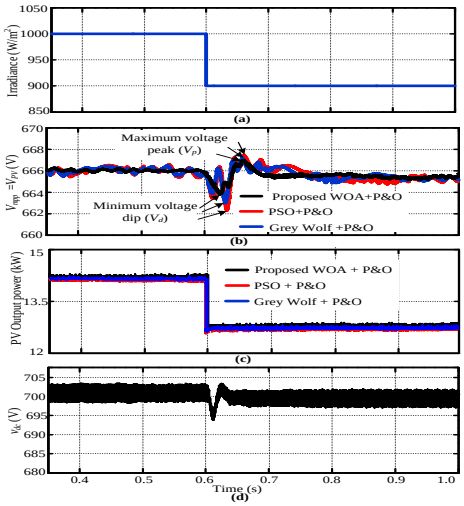

Figure 17: (a) Solar-irradiance, (b) V_{mpp} signal, (c) PV- array power, (d) DC-link voltage

FOREX Publication
Open Access | Rapid and quality publishing
International Journal of Electrical and Electronics Research (IJEER)
Case Study | Volume 11, Issue 2 | Pages 272-282 | e-ISSN: 2347-470X

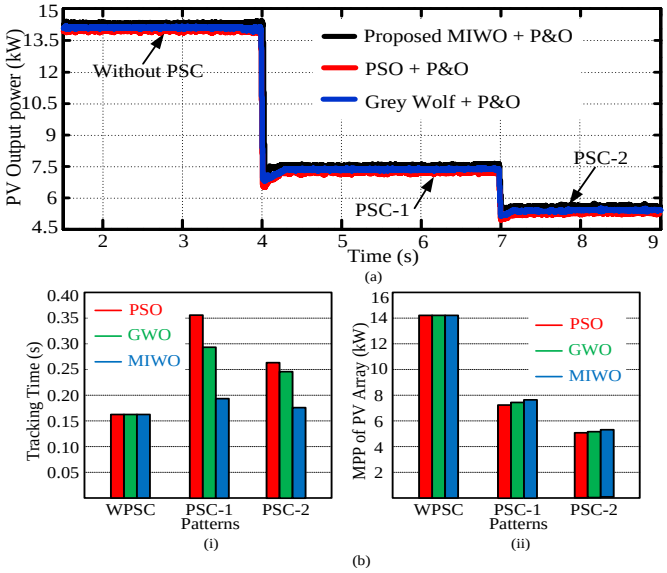

Figure 18: (a) Output power, (b)-(i) MPPT tracking time, (b)-(ii) MPPs

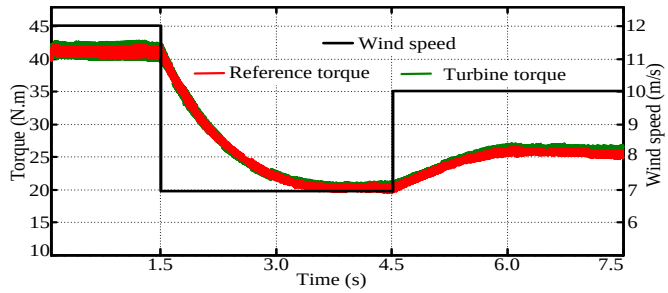

Figure 19: MPPT operation of wind turbine

Case-C: Responses of the system during unbalanced and nonlinear load

A 3-phase unbalanced (currents) load is connected at PCC that draws unbalanced current as illustrated in *figure 20(a)*. The voltage at PCC will be unbalanced voltages because of unbalanced voltage drops due to unbalanced currents. Unbalanced voltages may create several issues to connected loads at PCC, which lead to power quality problems. Moreover, these unbalanced voltages draw unbalanced currents from all inverters of wind farms as well as solar plants. For instance, these unbalanced currents of wind farm/solar plant inverters create second order oscillations, these oscillations will damage the wind turbine shaft [3] at the same time will produce heat on PV arrays. Thus, it is imperative in maintaining balanced three phase voltages at the Microgrid, irrespective of unbalanced currents. As unbalanced currents are noticed, the controller permits such oscillations through electrolyzer-FC inverter and then produce unbalanced currents to keep the balanced terminal voltages at PCC/Microgrid.

In this case study, considered unbalanced load at t =1sec. The injected 2nd wind farm's currents (balanced) and the voltages at PCC are depicted in *figure 20(b)* and *20(c)* respectively. Due to unbalanced currents, the generated oscillations in wind farm are mentioned in *20(e)* with the normal controller and proposed controller of inverter that is associated with electrolyzer-FC set.

It is noted that suggested controllers will control the second order oscillations. The generated three-phase balanced RMS voltages at PCC are in *figure 20(f)*.

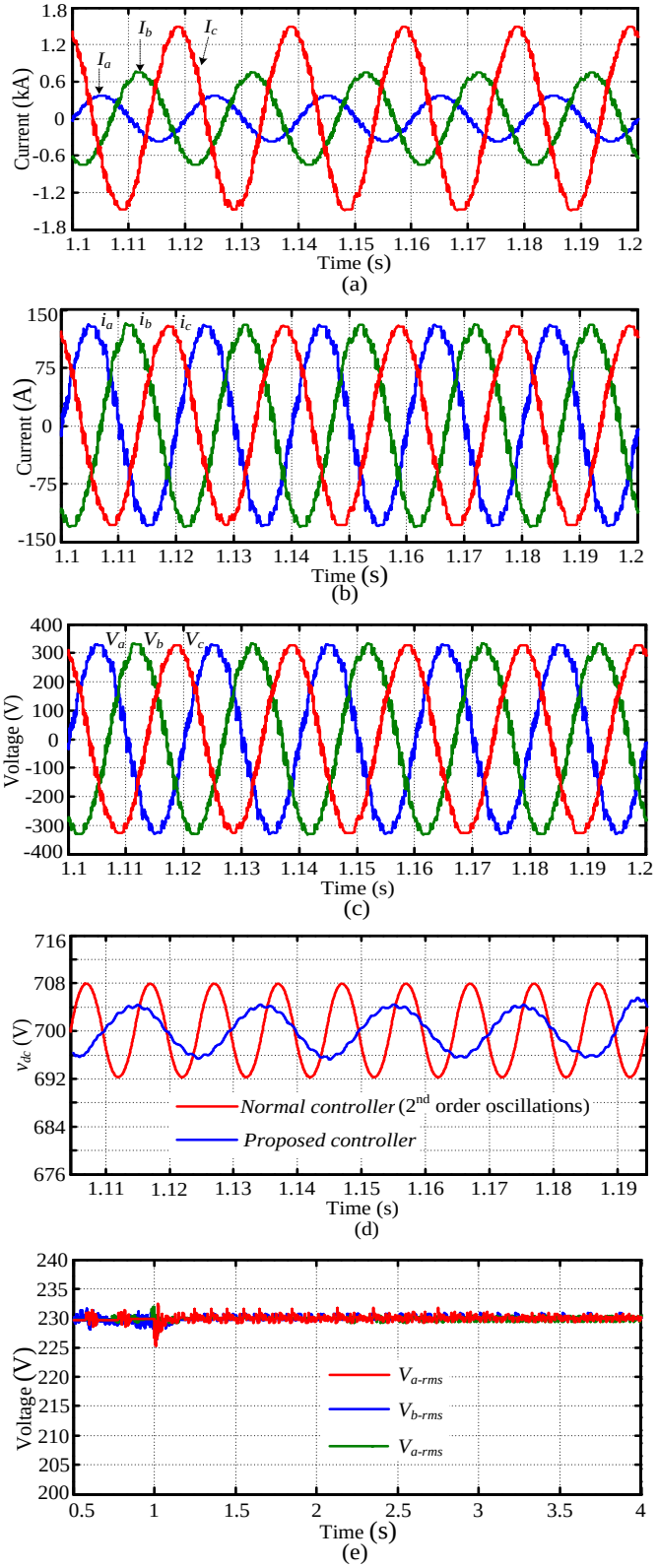

Figure 20: (a) unbalanced currents, (b) currents at wind farm-2, (c) voltages at PCC, (d) voltage at dc-link, (e) RMS phase voltages at PCC

FOREX Publication
Open Access | Rapid and quality publishing
International Journal of Electrical and Electronics Research (IJEER)
Case Study | Volume 11, Issue 2 | Pages 272-282 | e-ISSN: 2347-470X

The proposed controller is further tested under nonlinear loads. The ITD obtained from FFT of the voltage is depicted in *figure 21*. The values of positive and negative sequence of voltage are reported in *figure 22(a)* and *22(b)* respectively. The positive to negative voltage sequence factor is reported in *figure 22(c)* under the mixing of nonlinear and unbalanced loads at PCC. The positive to negative sequence factor value that was achieved is less than '1' percent, which suggests that further renewable energy sources may be added in the future.

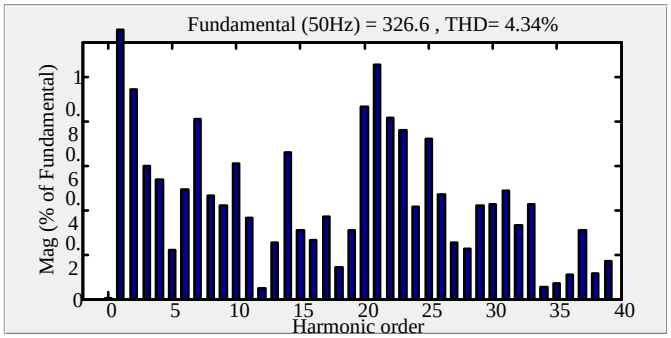

Figure 21: THD spectrum of phase voltage at PCC

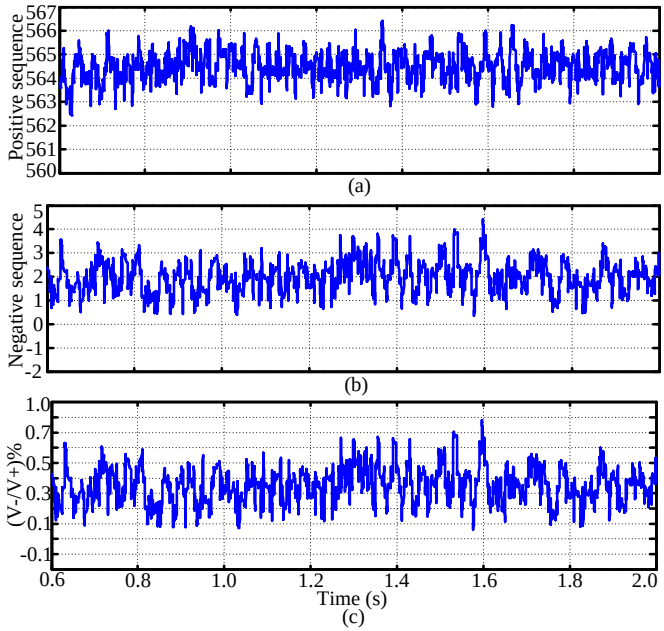

Figure 22: (a) positive sequence, (b) negative sequence, (c) ratio of positive-negative sequence voltage factor

Case-D: Operation with Electrolyzer and Fuel Cell

The battery controller will stop to charge the battery when SoC of battery reaches its upper limit (i.e., 80%). In this scenario, the power generated by wind farms and solar plants are considered more than the load demand. The load demand of 500 kW is considered at PCC in this situation and generation is about 1 MW. Hence, the surplus power is consumed by electrolyzer to produce oxygen and hydrogen which can easily be stored in tanks and can be utilized to generate electricity through FC when generation power is less than the load demand. The corresponding power diagram of all wind farms, solar plants, battery, FC and electrolyzer is shown in *figure 23*.

In similar manner, when load power is more than the total generation from wind farms and solar plants, the FC will start to produce electricity to maintain load demand. However, due to slow dynamics of FC, it cannot reach load demand instantaneously. During this time period, the battery will handle the load demand in transient time period and FC can handle the load demand in steady state. In this case 1.35 MW load is connected at PCC and the generation is at 1 MW. The corresponding powers are depicted in *figure 24*.

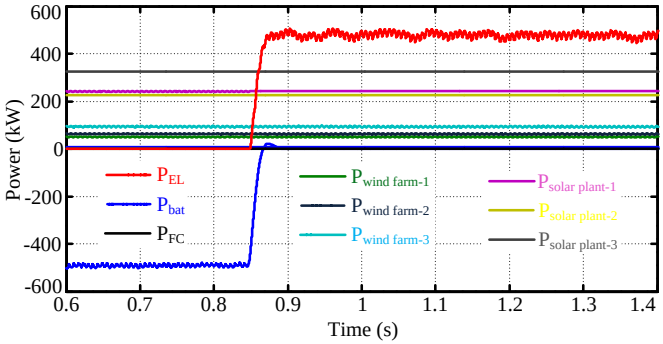

Figure 23: Powers under operation of electrolyzer

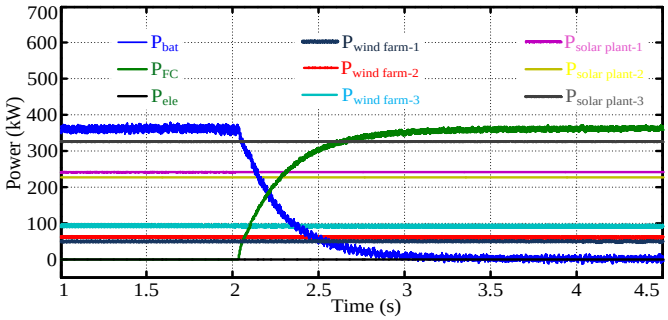

Figure 24: Powers under operation of Fuel Cell

7. CONCLUSION

An efficient energy management system is developed to provide an economical solution for the huge problem of power demand and emission without sacrificing the power quality for Microgrid based on Renewable Energy Sources. Hybrid MIWO-P&O algorithm is implemented for MPPT of PV system under PSCs. The designed controller was capable of transferring only active power to AC Microgrid while the reactive power being shared by all the PV inverters. Unbalanced load compensation was achieved with the help of FC-Electrolyzer concurrently. The results on OPAL-RT substantiate the effectiveness of the bestowed strategy and potentiality of the TS-Fuzzy based controller for the energy management system of renewable energy based standalone Microgrid utilizing Real time Simulator. Hardware in loop structure is implemented to demonstrate the viability of a more realistic simulation and controller testing. The positive to negative sequence of line-to-line voltage factor of less than '1'

International Journal of Electrical and Electronics Research (IJEER)
Case Study | Volume 11, Issue 2 | Pages 272-282 | e-ISSN: 2347-470X

has been maintained for all the controllers so that further integration of renewable sources is allowed to the AC Microgrid.

REFERENCES

[1] C. N. Bhende, S. Mishra and S. G. Malla, "Permanent Magnet Synchronous Generator-Based Standalone Wind Energy Supply System," in IEEE Transactions on Sustainable Energy, vol. 2, no. 4, pp. 361-373, Oct. 2011, doi: 10.1109/TSTE.2011.2159253.

[2] S.G. Malla, C.N. Bhende, Voltage control of stand-alone wind and solar energy system, International Journal of Electrical Power & Energy Systems, vol. 56, pp. 361-373, 2014, https://doi.org/10.1016/j.ijepes.2013.11.030.

[3] M. E. Haque, M. Negnevitsky, and K. M. Muttaqi, "A novel control strategy for a variable-speed wind turbine with a permanent-magnet synchronous generator," IEEE Trans. Ind. Appl., Vol. 46, no. 1, pp.331–339, Jan./Feb. 2010.

[4] J. Padulles, G. W. Ault and J. R. McDonald, "An integrated SOFC plant dynamic model for power systems simulation", Journal of Power Sources, Vol. 86, No. 1-2, pp. 495-500, March 2000.

[5] P.M. Dieguez, et al, "Thermal performance of commercial alkaline water electrolyzer: Experimental study and mathematical modeling", International Journal of Hydrogen Energy, Vol. 33, No. 24, pp. 7338-7354, Dec. 2008.

[6] S. Mohanty, B. Subudhi, and P. K. Ray, "A grey wolf assisted perturb & observe MPPT algorithm for a photovoltaic power system," IEEE Trans. Sustain. Energy, Vol. 32, no. 1, pp. 340–347, Mar. 2017.

[7] K. Sundareswaran, V. Kumar, and S. Palani, "Application of a combined particle swarm optimization and perturb and observe method for MPPT in PV systems under partial shading conditions," Renewable Energy, Vol. 75, pp. 308–317, Mar. 2015.

[8] C. Pradhan, et al, "Coordinated Power Management and Control of Standalone PV-Hybrid System With Modified IWO-Based MPPT," in IEEE Systems Journal, early access, doi: 10.1109/JSYST.2020.3020275.

[9] U. Akram, M. Khalid and S. Shafiq, "An Improved Optimal Sizing Methodology for Future Autonomous Residential Smart Power Systems," in IEEE Access, vol. 6, pp. 5986-6000, 2018, doi: 10.1109/ACCESS.2018.2792451.

[10] S. Rehman, et al., "Optimal Design and Model Predictive Control of Standalone HRES: A Real Case Study for Residential Demand Side Management," IEEE Access, vol. 8, pp. 29767-29814, 2020, doi:10.1109/ACCESS.2020.2972302.

[11] V. V. V. S. N. Murty and A. Kumar, "Optimal Energy Management and Techno-economic Analysis in Microgrid with Hybrid Renewable Energy Sources," in Journal of Modern Power Systems and Clean Energy, vol. 8, no. 5, pp. 929-940, September 2020, doi: 10.35833/MPCE.2020.000273.

[12] E. A. Al-Ammar et al., "Residential Community Load Management Based on Optimal Design of Standalone HRES With Model Predictive Control," in IEEE Access, vol. 8, pp. 12542-12572, 2020, doi: 10.1109/ACCESS.2020.2965250.

[13] U. K. Kalla, et al, "Adaptive Sliding Mode Control of Standalone Single-Phase Microgrid Using Hydro, Wind, and Solar PV Array-Based Generation," in IEEE Transactions on Smart Grid, vol. 9, no. 6, pp. 6806-6814, Nov. 2018, doi: 10.1109/TSG.2017.2723845.

[14] K. Kant, C. Jain and B. Singh, "A Hybrid Diesel-Wind-PV-Based Energy Generation System With Brushless Generators," in IEEE Transactions on Industrial Informatics, vol. 13, no. 4, pp. 1714-1722, Aug. 2017, doi: 10.1109/TII.2017.2677462.

[15] M. Rezkallah et al., "Comprehensive Controller Implementation for Wind-PV-Diesel Based Standalone Microgrid," in IEEE Transactions on Industry Applications, vol. 55, no. 5, pp. 5416-5428, Sept.-Oct. 2019, doi: 10.1109/TIA.2019.2928254.

[16] H. P. H. Anh, L. V. Truong and C. Van Kien, "Advanced Intelligent Fuzzy Control of Standalone PV-Wind-Diesel Hybrid System," 2019 International Conference on System Science and Engineering (ICSSE), 2019, pp. 129-135, doi: 10.1109/ICSSE.2019.8823562.

[17] M. S. Bisht and Sathans, "Fuzzy based intelligent frequency control strategy in standalone hybrid AC microgrid," 2014 IEEE Conference on Control Applications (CCA), 2014, pp. 873-878, doi: 10.1109/CCA.2014.6981446.

[18] H. U. Rahman Habib, S. Wang and M. T. Aziz, "PV-Wind-Battery Based Standalone Microgrid System with MPPT for Green and Sustainable Future," 2019 9th International Conference on Power and Energy Systems (ICPES), 2019, pp. 1-6, doi: 10.1109/ICPES47639.2019.9105395.

[19] V. Papadopoulos, J. Knockaert, C. Develder and J. Desmet, "Techno-economic study of hydrogen production using PV, wind power and battery storage," 2019 IEEE PES Innovative Smart Grid Technologies Europe (ISGT-Europe), 2019, pp. 1-5, doi: 10.1109/ISGTEurope.2019.8905629.

[20] A. Sathyan, K. Anthony and S. Al-Hallaj, "Hybrid wind/PV/fuel cell generation system," 2005 IEEE Vehicle Power and Propulsion Conference, 2005, pp. 6 pp.-, doi: 10.1109/VPPC.2005.1554604.

[21] S. Dey, R. Dash and S. C. Swain, "Fuzzy based optimal load management in standalone hybrid solar PV/Wind/Fuel Cell generation system," 2015 Communication, Control and Intelligent Systems (CCIS), 2015, pp. 486-490, doi: 10.1109/CCIntelS.2015.7437965.

[22] P. García, et al, "ANFIS-Based Control of a Grid-Connected Hybrid System Integrating Renewable Energies, Hydrogen and Batteries," in IEEE Transactions on Industrial Informatics, vol. 10, no. 2, pp. 1107-1117, May 2014, doi: 10.1109/TII.2013.2290069.

[23] Abdullah Al-Sharafi, et al, "Techno-economic analysis and optimization of solar and wind energy systems for power generation and hydrogen production in Saudi Arabia", Renewable and Sustainable Energy Reviews, Volume 69, 2017, Pages 33-49, https://doi.org/10.1016/j.rser.2016.11.157.